

Nonuniform variation of the radiative lifetimes of bound excited states along the Mg isoelectronic sequence

T. N. Chang and Rong-qi Wang

Department of Physics, University of Southern California, Los Angeles, California 90089-0484

(Received 30 January 1991)

We present the result of a simple nonvariational configuration-interaction calculation for the energy levels and the radiative lifetimes of the Mg isoelectronic sequence. Emphasis is placed on the nonuniform variation of the radiative lifetimes for a series of singly excited states along the isoelectronic sequence due to the strong configuration mixing between the singly excited series and the doubly excited perturbers. The energy contributions from the bound-continuum type of configurations corresponding to the combination of negative- and positive-energy orbitals for the two valence electrons in a divalent atom are examined in detail within the frozen-core Hartree-Fock approximation. Comparisons with existing theoretical and experimental data are also presented.

I. INTRODUCTION

The isoelectronic smoothing of the excitation energies and the oscillator strengths for the low-lying excited states often helps to identify the incorrect experimental assignments for atomic transitions [1,2]. It can also lead to a simple quantitative procedure for interpolation (or, even for extrapolation) of the missing spectroscopy data when it is combined with the use of properly established theoretical analysis, such as the Z^{-1} perturbation expansion approach [3–6]. On the other hand, for transitions involving strongly correlated higher excited states, the presence of *local* irregularities in oscillator strengths as the nuclear charge Z varies along the isoelectronic sequence [7–12] could make the application of such a smoothing procedure difficult. For divalent atoms, as Z increases along an isoelectronic sequence, the nuclear attraction for a doubly excited state could become stronger than that for a singly excited state due to a less complete mutual screening between two simultaneously excited electrons than the screening experienced by the outer electron from a radially separated inner electron. As a result, some of the prominent autoionization structures, usually located above the first ionization threshold for a neutral atom, will *plunge* [8] into the discrete spectrum of ionic systems. The nearly degenerate overlapping between the doubly and singly excited bound states may lead to strongly *localized* configuration mixing, which manifests itself through the redistribution of the oscillator strengths among transitions from a series of singly excited states due to the presence of the doubly excited perturbers [7]. Anomalies in the fine-structure-level splittings have also been observed in divalent atoms due to the strong interaction between the singly and doubly excited configurations [9]. Another example includes the J -dependent lifetimes in Mg-like ions due to the singlet-triplet mixing, again, resulting from the configuration interaction [10–12]. Such irregularities diminish eventually at high- Z limit where states are grouped together in terms of the principal quantum numbers.

Advances in recent ion source technology, such as EBIS (electron beam ion source, e.g., see Briand *et al.*

[13]) or EBIT (electron beam ion trap, e.g., see Marrs *et al.* [14]), have opened up opportunities for systematic structure studies for atomic ions. In particular, detailed *quantitative* analysis can be carried out if the ion sources are prepared in a controlled environment with more sophisticated ion trap and laser cooling techniques [15,16]. In addition, the doubly excited bound and autoionization states of neutral and ionic systems can also be generated and studied following the double electron capture process by low-energy ions colliding with neutral He or other rare-gas atoms [17]. These newly available experimental possibilities should help in the immediate future to assess the accuracy of quantitative estimation in any theoretical attempt to identify the presence of the spectroscopy irregularities discussed earlier for the low to intermediate Z members of an isoelectronic sequence.

In this paper, we extend our recent studies [7,18–20], on the effect of configuration interaction to the energy levels, the oscillator strengths, and the radiative lifetimes of the bound excited states, to few atomic ions (including Al II, Si III, P IV, and S V) of the Mg isoelectronic sequence. Emphasis will be given to the nonuniform variation of the radiative lifetimes for the singly excited series along the isoelectronic sequence due to the presence of the doubly excited perturbers. In Sec. II we briefly summarize the simple nonvariational configuration-interaction (CI) procedure [7,18–21] employed in the present calculation. In Sec. III we examine the effect on the energy levels due to the addition of positive-energy (i.e., continuum) one-electron orbitals, which is expanded in terms of B -spline function [20,22,23], to a discretized finite CI basis set. Finally, the nonuniform variation of the calculated radiative lifetimes for the $3snd\ ^1D$ series along the Mg isoelectronic sequence due to the strong mixing between the $3sd$ and $3pp$ configuration series will be discussed.

II. CALCULATIONAL PROCEDURE

Briefly, for a divalent atom, the energy eigenvalue and its corresponding eigenvector, for a bound excited state

of a given symmetry (i.e., total spin S and total orbital angular momentum L), are calculated by diagonalizing a Hamiltonian matrix constructed from an L^2 finite basis set with one-particle radial functions subject to a frozen-core Hartree-Fock (FCHF) potential corresponding to a 1S closed shell core. The basis set consists of a number of configuration series nll' discussed in detail earlier [7,18–21]. The one-particle radial functions are expanded in terms of a set of B splines confined between $r=0$ and a maximum radius $r=R$ for a finite sphere [20,22,23]. An energy eigenvalue calculated from this simple nonvariational CI procedure is denoted as $E_{n_i l_i n_0 l_0}$ if the corresponding eigenstate is dominated by a two-electron configuration ($n_i l_i n_0 l_0$) with the inner valence electron in an $n_i l_i$ orbital and the outer valence electron in an $n_0 l_0$ orbital. Within the FCHF approximation, the calculated energy $E_{n_i l_i n_0 l_0}$ equals the energy *difference* between the eigenstate $n_i l_i n_0 l_0 (^{2S+1}L)$ and the ionization threshold (at zero energy) corresponding to the removal of both valence electrons. The energy eigenvalue $E_{n_i l_i n_0 l_0}$ in Ry units can be expressed in terms of the *quantum defect* $\delta_{n_i l_i}$, or its corresponding effective quantum number $\nu_{n_i l_i} = n_0 - \delta_{n_i l_i}$ leading to the $n_i l_i$ threshold of the atomic ion, by

$$E_{n_i l_i n_0 l_0}(N, Z) = -E_{n_i l_i}^I(N-1, Z) - \frac{Z_e^2}{\nu_{n_i l_i}^2}, \quad (1)$$

where N is the total number of electrons in the divalent atom, $Z_e = Z - N + 1$ is the effective nuclear charge, and $E_{n_i l_i}^I(N-1, Z)$ is the ionization energy required to remove the $n_i l_i$ electron from the residual atomic ion of $N-1$ electrons.

The radiative lifetime τ_b of an excited state $|b\rangle$ is calculated by taking the sum over the transition probabilities A_{ba} of all emissions from the upper state $|b\rangle$ to a lower state $|a\rangle$, i.e.,

$$\frac{1}{\tau_b} = \sum_a A_{ba}. \quad (2)$$

In the present study, only the allowed dipole transitions are included and the numerical results from our calculation should be considered as the upper bound for the radiative lifetime. The transition probability A_{ba} , given in units of nsec^{-1} (i.e., 10^9 sec^{-1}), is expressed in terms of the oscillator strength for emission f_{ab}^e by [18,24]

$$A_{ba} = 8.0323(\Delta E_{ba})^2 |f_{ab}^e|, \quad (3)$$

where the excitation energy ΔE_{ba} is calculated in Ry units. The oscillator strength f_{ab}^e for an emission from an upper state $|b\rangle$ to a lower state $|a\rangle$ is related to the oscillator strength f_{ba}^{abs} for an absorption from a lower state $|a\rangle$ to an upper state $|b\rangle$ by

$$f_{ab}^e = - \left(\frac{2L_a + 1}{2L_b + 1} \right) f_{ba}^{\text{abs}}. \quad (4)$$

The calculational procedure for the oscillator strengths employed in the present simple CI procedure has been presented in detail elsewhere [20,25].

III. RESULTS AND DISCUSSIONS

Unlike our earlier calculation [7], which is carried out in a simple CI approach similar to the truncated diagonalization method [21,26] (TDM), the use of discretized finite basis has allowed us to include effectively the CI contributions from the positive-energy orbitals in the present calculation. The energy corrections due to the multielectron interaction between various combinations of bound (negative-energy) and continuum (positive-energy) orbitals have been examined in detail recently for the highly correlated H^- atom [27]. In particular, we have shown that the continuum-continuum type of configurations contribute significantly to the electron affinity of H^- . To illustrate the relative energy contributions from various combinations of electron configurations for the two outer electrons, a detailed breakdown of the calculated energies in terms of the quantum defects for the $3sns \ ^1S$ series of Al II is shown in Fig. 1. As expected, the calculated energies are substantially different from the observed values when our calculation

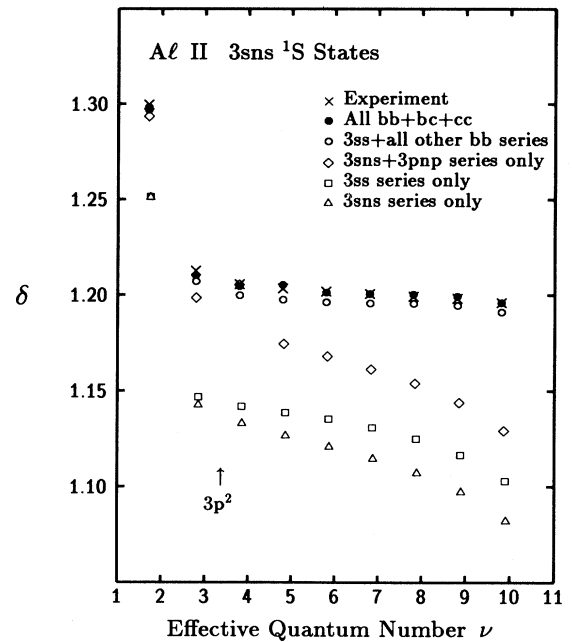


FIG. 1. A breakdown in energy contribution calculated with different combinations of configurations for the singly excited $3sns \ ^1S$ series of Al II. The energy is expressed in terms of quantum defect δ which varies as a function of effective quantum number ν . The experimental data are taken from Ref. 28. The $3p^2 \ ^1S$ state indicated by the arrow is plotted at an effective quantum number calculated with respect to the $3s$ ionization threshold.

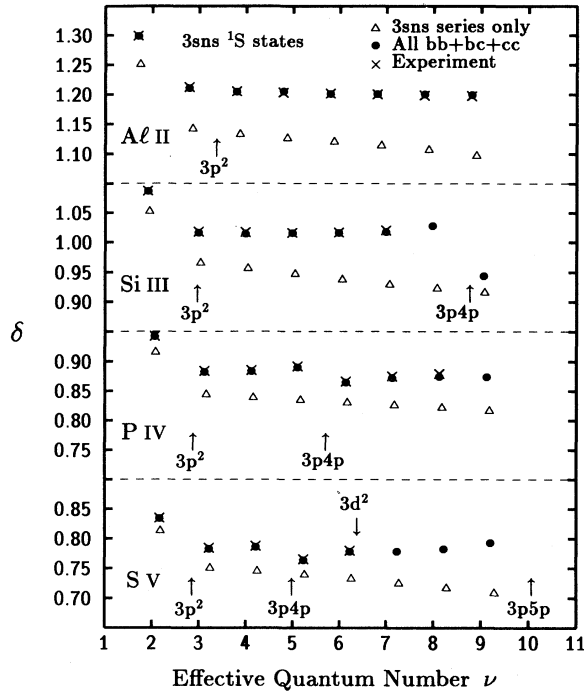


FIG. 2. Variations of quantum defects for the singly excited $3sns\ ^1S$ series for Al II, Si III, P IV, and S V. The experimental data are taken from Refs. [28]–[31]. The doubly excited states indicated by arrows are plotted at effective quantum numbers calculated with respect to the $3s$ ionization threshold.

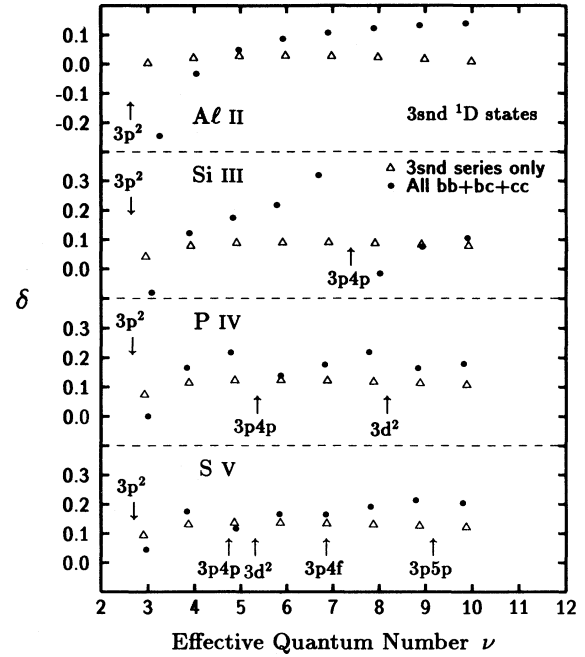


FIG. 4. Variations of quantum defects for the singly excited $3snd\ ^1D$ series for Al II, Si III, P IV, and S V. The doubly excited states indicated by arrows are plotted at effective quantum numbers calculated with respect to the $3s$ ionization threshold.

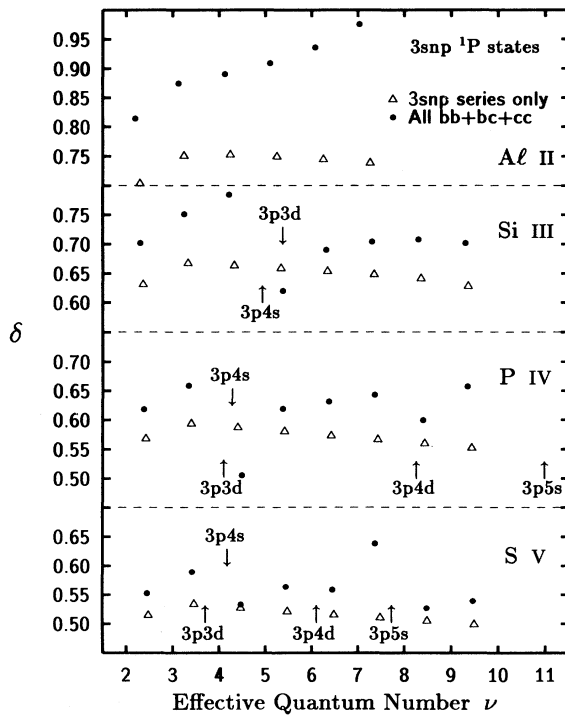


FIG. 3. Variations of quantum defects for the singly excited $3snp\ ^1P$ series for Al II, Si III, P IV, and S V. The doubly excited states indicated by arrows are plotted at effective quantum numbers calculated with respect to the $3s$ ionization threshold.

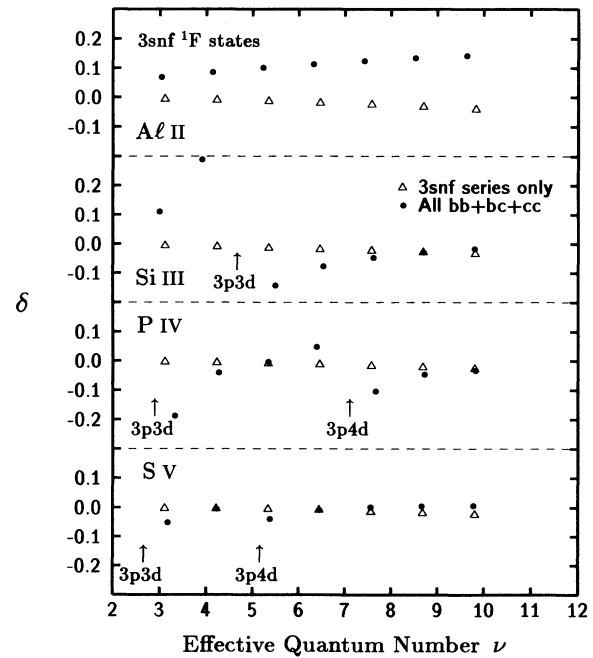


FIG. 5. Variations of quantum defects for the singly excited $3snf\ ^1F$ series for Al II, Si III, P IV, and S V. The doubly excited states indicated by arrows are plotted at effective quantum numbers calculated with respect to the $3s$ ionization threshold.

includes only the $3sns$ configurations corresponding to the negative-energy orbitals. The energy correction due to the addition of bound-continuum type of configurations included in the $3ss$ configuration series is small but significant, as shown by the difference between the quantum defects corresponding to the $3ss$ series and $3sns$ series, respectively. Similar to our earlier conclusion, the dominant energy correction can be attributed to the strong interaction between the bound-bound type of configurations corresponding to the $3sns$ and $3pnp$ series. In fact, for the ground and the low-lying excited states, the calculated energies are already very close to the observed values when the bound-bound type of CI contributions from the $3sns$ and $3pnp$ series are included. For the higher excited states, the contributions from other configuration series are clearly required. However, unlike H^- , the contribution from the continuum-continuum type of configurations is very small for heavier divalent atoms. The calculated energies generally agree to the observed values to 10^{-3} Ry and our calculated quantum defects are in very close agreement with the experiment as shown in Fig. 1.

The energy corrections for all singly excited $3snl\ ^1L$ series (for $L=0-3$) for Al II, Si III, P IV, and S V due to the presence of doubly excited perturbers are illustrated

by the changes in quantum defects δ shown in Figs. 2–5. The calculated energies, with limited contribution from the $3snl$ bound only configuration series, are also plotted in terms of their quantum defects for comparison. As expected, the change in quantum defect, from the $3snl$ only to the complete calculation, decreases as Z increases due to the strong presence of the nuclear attraction. In addition, the quantum defect itself decreases due to the increasingly more complete screening experienced by the outer electron as Z increases. Except for the 1P series, the variation in quantum defects due to the presence of neighboring doubly excited perturbers also diminishes as Z increases. This is due to the cancellation between energy corrections resulting from the doubly excited perturbers, which belong to the *same* configuration series but locate on the opposite sides of the individual excited state. For the 1P series, the corrections due to two *different* configuration series (i.e., $3pns$ and $3pnd$) differ significantly. As a result, large variations in quantum defects remain evident even for S V. By including the CI contributions from the bound-continuum type of configurations in the present calculation, the agreement between the theoretical quantum defects and their corresponding experimental values has improved significantly over our earlier calculation [7]. The overall agreement

TABLE I. The excitation energies in a.u. for the excited states of Al II. The energy for the $3s\ ^2S$ ground state from the present calculation is $-1.735\ 98$ a.u., which is slightly above the observed value of $-1.737\ 37$ a.u. from Ref. [28].

State	Expt. ^a	Present	Ref. [32]	Theory			Ref. [36]
				Ref. [33]	Ref. [34]	Ref. [35]	
$3s4s\ ^1S$	0.4312	0.4335	0.4301	0.4314			0.4281
$3p^2\ ^1S$	0.5087	0.5088	0.5084	0.5123		0.5028	0.5028
$3s5s\ ^1S$	0.5530	0.5517	0.5484				
$3s6s\ ^1S$	0.6050	0.6035	0.6002				
$3s3p\ ^1P$	0.2727	0.2720	0.2735	0.2735		0.2710	0.2709
$3s4p\ ^1P$	0.4872	0.4858	0.4830	0.4807			
$3s5p\ ^1P$	0.5735	0.5721	0.5703				
$3s6p\ ^1P$	0.6148	0.6134	0.6146				
$3p^2\ ^1D$	0.3895	0.3888	0.3836	0.3818		0.3793	0.3795
$3s3d\ ^1D$	0.5016	0.5007	0.5009	0.4975		0.4951	0.4958
$3s4d\ ^1D$	0.5686	0.5675	0.5661				
$3s4f\ ^1F$	0.5625	0.5611	0.5775		0.5544		
$3s4s\ ^3S$	0.4159	0.4144	0.4117	0.4103			0.4098
$3s5s\ ^3S$	0.5472	0.5456	0.5426				
$3s6s\ ^3S$	0.6024	0.6008	0.5978				
$3s3p\ ^3P$	0.1709	0.1708	0.1671	0.1666			0.1646
$3s4p\ ^3P$	0.4805	0.4793	0.4756	0.4719			
$3p4s\ ^3P$	0.6648	0.6636	0.6650				
$3s3d\ ^3D$	0.4354	0.4341	0.4326	0.4321	0.4285		0.4288
$3s4d\ ^3D$	0.5535	0.5521	0.5531				
$3s4f\ ^3F$	0.5623	0.5609	0.5774		0.5540		0.5584
$3s5f\ ^3F$	0.6080	0.6067					0.6036
$3s6f\ ^3F$	0.6313	0.6300					0.6282
$3p3d\ ^3F$	0.6430	0.6417	0.6333		0.6333		0.6323
$3s7f\ ^3F$	0.6528	0.6515					0.6432
$3s8f\ ^3F$	0.6613	0.6599					0.6536
$3s9f\ ^3F$	0.6675	0.6661					0.6592
$3s10f\ ^3F$	0.6721	0.6707					0.6639

^aReference [28].

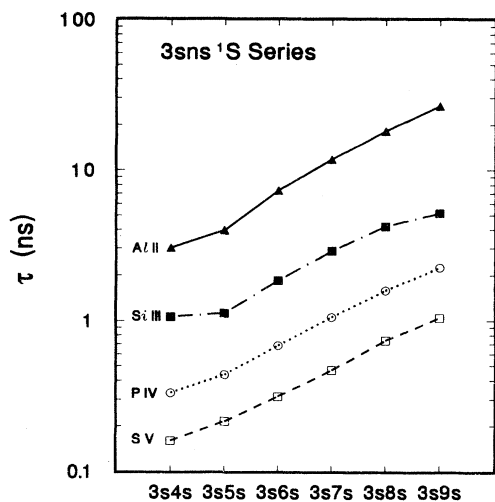


FIG. 6. Variation of radiative lifetime τ along the singly excited $3sns \ ^1S$ series for Al II, Si III, P IV, and S V.

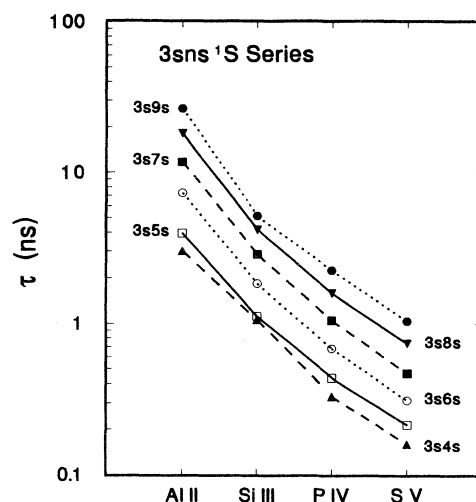


FIG. 7. Variation of radiative lifetime τ along the Mg isoelectronic sequence for the singly excited $3sns \ ^1S$ series.

TABLE II. The excitation energies in a.u. for the excited states of Si III. The energy for the $3s \ ^2S$ ground state from the present calculation is -2.88772 a.u., which is slightly above the observed value of -2.88977 a.u. from Ref. [29].

State	Expt. ^a	Present	Ref. [32]	Ref. [34]	Theory			
					Ref. [35]	Ref. [8]	Ref. [37]	Ref. [36]
$3p \ ^2S$	0.6992	0.6994	0.7051		0.6931		0.7044	0.6940
$3s4s \ ^1S$	0.7248	0.7236	0.7222				0.7180	0.7178
$3s5s \ ^1S$	0.9472	0.9455	0.9438					
$3s6s \ ^1S$	1.0496	1.0477	1.0476					
$3p4p \ ^1S$	1.1800	1.1695	1.1692					
$3s3p \ ^1P$	0.3776	0.3766	0.3834		0.3769		0.3797	0.3770
$3s4p \ ^1P$	0.8041	0.8023	0.8016				0.7946	
$3s5p \ ^1P$	0.9775	0.9755	0.9746					
$3p4s \ ^1P$	1.0420	1.0405	1.0411					
$3p3d \ ^1P$	1.0679	1.0700	1.0728					
$3s6p \ ^1P$	1.0751	1.0733	1.0793					
$3p \ ^2D$	0.5569	0.5562	0.5531					
$3s3d \ ^1D$	0.7553	0.7545	0.7605		0.5445		0.5515	0.5451
$3s4d \ ^1D$	0.9310	0.9295	0.9313		0.7504		0.7575	0.7543
$3p4p \ ^1D$	1.1297	1.1452	1.1383					
$3s4f \ ^1F$	0.9333	0.9313	0.9318		0.9214			
$3s5f \ ^1F$	1.0276	1.0260					1.0173	
$3p3d \ ^1F$	1.0726	1.0714	1.0618				1.0636	
$3s4s \ ^3S$	0.6989	0.6969	0.6957					
$3s5s \ ^3S$	0.9394	0.9373	0.9360				0.6880	0.6909
$3s6s \ ^3S$	1.0463	1.0441	1.0435					
$3p4p \ ^3S$	1.1335	1.1315	1.1299					
$3s3p \ ^3P$	0.2414	0.2414	0.2398				0.2368	0.2340
$3s4p \ ^3P$	0.7987	0.7972	0.7954				0.7860	
$3s5p \ ^3P$	0.9796	0.9778	0.9772					
$3p3d \ ^3P$	0.9853	0.9844	0.9841					
$3p4s \ ^3P$	1.0328	1.0313	1.0317					
$3s6p \ ^3P$	1.0682	1.0662	1.0675					
$3s3d \ ^3D$	0.6512	0.6496	0.6510	0.6439			0.6468	0.6447
$3s4d \ ^3D$	0.9186	0.9166	0.9195					
$3p4p \ ^3D$	1.1130	1.1141	1.1106					
$3p3d \ ^3F$	0.9070	0.9056	0.9046	0.8917				
$3s4f \ ^3F$	0.9554	0.9529	0.9560	0.9437				

^aReference [29].

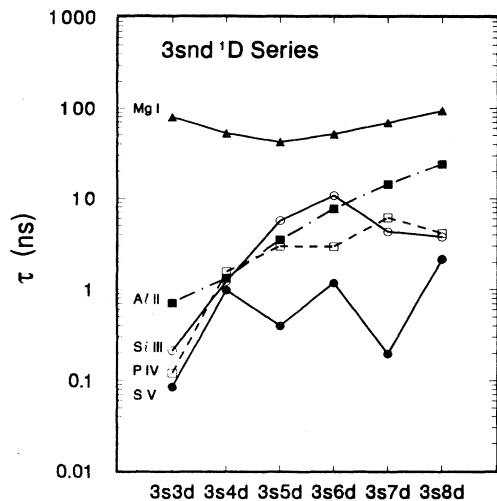


FIG. 8. Variation of radiative lifetime τ along the singly excited $3snd\ ^1D$ series for Mg I, Al II, Si III, P IV, and S V.

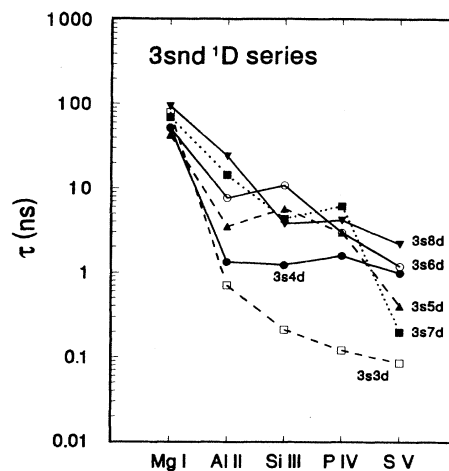


FIG. 9. Variation of radiative lifetime τ along the Mg isoelectronic sequence for the singly excited $3snd\ ^1D$ series.

TABLE III. The excitation energies in a.u. for the excited states of P IV. The energy for the $3s\ ^2S$ ground state from the present calculation is $-4.277\ 50$ a.u., which is slightly above the observed value of $-4.280\ 23$ a.u. from Ref. [30].

State	Expt. ^a	Present	Ref. [10]	Ref. [32]	Theory Ref. [38]	Ref. [34]	Ref. [35]	Ref. [8]
$3p\ ^2S$	0.8866	0.8869		0.8945	0.8861		0.8807	
$3s4s\ ^1S$	1.0662	1.0651		1.0622	1.0636			
$3s5s\ ^1S$	1.4179	1.4159		1.4126				
$3s6s\ ^1S$	1.5838	1.5815		1.5786				
$3p4p\ ^1S$	1.6390	1.6373	1.6513	1.6380				
$3s3p\ ^1P$	0.4793	0.4773		0.4862	0.4807		0.4790	
$3s4p\ ^1P$	1.1733	1.1711	1.1678	1.1692	1.1641			
$3p3d\ ^1P$	1.3992	1.4007	1.4120	1.4073	1.4058			1.3996
$3p4s\ ^1P$	1.4439	1.4419		1.4389				
$3s5p\ ^1P$	1.4939	1.4917		1.4920				
$3p\ ^2D$	0.7206	0.7200		0.7161	0.7107		0.7061	
$3s3d\ ^1D$	0.9985	0.9982		1.0067	1.0048		0.9952	
$3s4d\ ^1D$	1.3456	1.3438		1.3460	1.3401			
$3p4p\ ^1D$	1.6056	1.6039		1.6037				
$3d\ ^2D$	1.7738	1.7665	1.7734	1.7941				1.7533
$3p3d\ ^1F$	1.3228	1.3210	1.3175	1.3247				1.3108
$3s4f\ ^1F$	1.4326	1.4316		1.4399				1.4243
$3p4d\ ^1F$	1.7587	1.7277	1.7343					
$3s4s\ ^3S$	1.0338	1.0315		1.0294	1.0305			
$3s5s\ ^3S$	1.4084	1.4059		1.4030				
$3s6s\ ^3S$	1.5787	1.5761		1.5731				
$3p4p\ ^3S$	1.5911	1.5885	1.5939	1.5868				
$3s3p\ ^3P$	0.3116	0.3117		0.3091	0.3036			
$3s4p\ ^3P$	1.1693	1.1679	1.1619	1.1650	1.1582			
$3p3d\ ^3P$	1.2810	1.2796	1.2815	1.2811	1.2771			
$3p4s\ ^3P$	1.4496	1.4480		1.4445				
$3s5p\ ^3P$	1.4694	1.4668		1.4655				
$3s6p\ ^3P$	1.6116	1.6092		1.6075				
$3p4d\ ^3P$	1.7557	1.7532	1.7589					
$3s3d\ ^3D$	0.8630	0.8609		0.8629	0.8610			
$3s4d\ ^3D$	1.3361	1.3338		1.3361	1.3290			
$3p4p\ ^3D$	1.5715	1.5690	1.5736	1.5686				
$3p3d\ ^3F$	1.1952	1.1938	1.1882	1.1912		1.1773		
$3s4f\ ^3F$	1.3853	1.3810		1.3832		1.3706		
$3p4d\ ^3F$	1.7383	1.7372	1.7326					

^aReference [30].

between theory and experiment [28–31] for the 1P , 1D , and 1F series (not shown) is about the same as that shown in Fig. 2 for the 1S series. The arrows indicating the doubly excited perturbers shown in Figs. 2–5 are plotted at effective quantum numbers calculated with respect to the $3s$ ionization threshold according to Eq. (1). The excitation energies for selected excited states measured from the calculated $3s^2\ ^1S$ ground state are compared with a few other theoretical calculations [8,10,11,32–40] in Tables I–IV. We should note that some of the listed theoretical results [8,11,34–36,40] compare better with the observed data if they are expressed in terms of the term values with respect to the first ionization threshold. Our theoretical results are also in overall close agreement with the observed data [28–31].

The radiative lifetimes for the low-lying excited states

usually decrease monotonically along the Mg isoelectronic sequence. For instance, Froese Fischer and Godefroid [35] have shown that the lifetimes due to the $\Delta n=0$ cascades for the $n=3$ singlet states can be expressed in terms of a fairly smooth function of Z^{-1} . In addition, the radiative lifetimes for a series of singly excited $3snl\ ^1,^3L$ states near the neutral end of the isoelectronic sequence often increase monotonically as the effective quantum number ν increases. An effective isoelectronic smoothing procedure can be carried out if these two basic criteria are satisfied. For the $3sns\ ^1S$ series, our calculated radiative lifetimes, shown in Figs. 6 and 7, are found to follow these two general trends, at least, qualitatively. The crossing between the doubly excited $3p^2\ ^1S$ and the singly excited $3s4s\ ^1S$ states from Al II to Si III, shown in Fig. 2, is responsible for the minor slowdown in the increase of

TABLE IV. The excitation energies in a.u. for the excited states of S V. The energy for the $3s^2\ ^1S$ ground state from the present calculation is -5.90056 a.u., which is slightly above the observed value of -5.90378 a.u. from Ref. [31].

State	Expt. ^a	Present	Theory					
			Ref. [10]	Ref. [32]	Ref. [39]	Ref. [11]	Ref. [35]	Ref. [40]
$3p^2\ ^1S$	1.0723	1.0728		1.0837	1.0752	1.0757		1.0891
$3s4s\ ^1S$	1.4585	1.4574		1.4555	1.4485			1.4579
$3s5s\ ^1S$	1.9629	1.9608		1.9584				1.9608
$3p4p\ ^1S$	2.1530	2.1516	2.1679	2.1526				
$3s6s\ ^1S$	2.2116	2.2088		2.2085				
$3s3p\ ^1P$	0.5794	0.5771		0.5889	0.5824		0.5787	0.5905
$3s4p\ ^1P$	1.5926	1.5899	1.5878	1.5895	1.5791	1.5848		1.5937
$3p3d\ ^1P$	1.7646	1.7300	1.7480	1.7419	1.7339		1.7242	1.7498
$3p4s\ ^1P$	1.9343	1.9318		1.9314	1.9388			1.9356
$3s5p\ ^1P$	2.0409	2.0382		2.0389				
$3s6p\ ^1P$	2.2450	2.2416		2.2430				
$3p4d\ ^1P$	2.3137	2.3235	2.3353					
$3p^2\ ^1D$	0.8827	0.8827		0.8801	0.8722	0.8757		0.8883
$3s3d\ ^1D$	1.2334	1.2332		1.2467	1.2364	1.2393		1.2513
$3s4d\ ^1D$	1.8117	1.8095		1.8142				1.8146
$3p4p\ ^1D$	2.0969	2.0950	2.0967	2.0936	2.0823			2.0998
$3p3d\ ^1F$	1.6716	1.6709	1.6842	1.6805	1.6715		1.6578	
$3s4f\ ^1F$	1.9045	1.9029		1.9117	1.9031			
$3p4d\ ^1F$	2.2896	2.2922	2.3037					
$3s4s\ ^3S$	1.4197	1.4172		1.4162	1.4069	1.4132		
$3s5s\ ^3S$	1.9522	1.9493		1.9476				
$3p4p\ ^3S$	2.0955	2.0927	2.0990	2.0925				
$3s6s\ ^3S$	2.2037	2.2072		2.1999				
$3s3p\ ^3P$	0.3817	0.3823		0.3802	0.3750			
$3p3d\ ^3P$	1.5744	1.5732	1.5791	1.5784	1.5646			
$3s4p\ ^3P$	1.5917	1.5900	1.5858	1.5887	1.5775			
$3p4s\ ^3P$	1.9200	1.9191		1.9170	1.9388			
$3s5p\ ^3P$	2.0296	2.0266		2.0257				
$3s6p\ ^3P$	2.2329	2.2406		2.2414				
$3p4d\ ^3P$	2.2829	2.3080	2.3180					
$3s3d\ ^3D$	1.0705	1.0682		1.0734	1.0620	1.0702		
$3s4d\ ^3D$	1.8045	1.8019		1.8069	1.7945			
$3p4p\ ^3D$	2.0628	2.0603	2.0638	2.0591	2.0537			
$3p4f\ ^3D$		2.3691	2.3772					
$3p3d\ ^3F$	1.4748	1.4736	1.4720	1.4737	1.4588			
$3s4f\ ^3F$	1.8723	1.8693		1.8745	1.8584			
$3p4d\ ^3F$	2.2679	2.2878	2.2922					

^aReference [31].

the radiative lifetimes for Al II and Si III near $3s5s\ ^1S$ as shown in Fig. 6.

For excited states, which are strongly affected by the configuration mixing between the singly and doubly excited configurations, the variation of their radiative lifetimes could be highly irregular as shown in Figs. 8 and 9 for the excited $3snd\ ^1D$ series. The radiative lifetime for the singly excited $3snd\ ^1D$ series of neutral Mg is known to be dominated by the doubly excited $3pp\ ^1D$ series located at energies near and above the first ionization threshold [18]. The effect due to the $3p^2\ ^1D$ state for other members in the Mg sequence remains strong, but with the $3p^2\ ^1D$ state located below the $3s3d\ ^1D$ state (see Fig.

4), the radiative lifetime for the lowest $3s3d\ ^1D$ state is reduced uniformly when Z increases as shown in Fig. 9. The reduction in the radiative lifetime for Si III $3s7d$ and $3s8d\ ^1D$ states shown in Fig. 8 can be easily linked to the presence of the $3p4p\ ^1D$ state between $3s7d$ and $3s8d\ ^1D$ states shown in Fig. 4. A near zero increase in lifetime also exists between the $3s5d$ and $3s6d\ ^1D$ states for P IV due to the same $3p4p\ ^1D$ perturber. In addition, the lifetime for the $3s8d\ ^1D$ state of P IV is reduced slightly due to the neighboring $3d^2\ ^1D$ state located on the higher-energy side shown in Fig. 4. More drastic nonuniform variation of the radiative lifetimes is shown in Fig. 8 for S V due to the extensive overlapping of the singly excited

TABLE V. The radiative lifetimes for a few selected low-lying excited states for Al II, Si III, P IV, and S V.

State	Experiment	Present	Ref. [41]	Theory Ref. [35]	Ref. [42]	Others
Al II	$3s4s\ ^1S$	3.05	3.04			
Al II	$3s3p\ ^1P$	0.68 ± 0.1^a 0.72 ± 0.11^b	0.70		0.70	
Al II	$3s4p\ ^1P$		10.76	9.33		
Al II	$3s3d\ ^1D$	0.71 ± 0.03^b	0.712		0.75	
Al II	$3s4s\ ^3S$	2.1 ± 0.2^c	1.365	1.35		
Al II	$3s3d\ ^3D$	0.77 ± 0.1^c 0.86 ± 0.05^b	0.822			
Al II	$3s4f\ ^3F$	6.4 ± 0.5^d	4.22			3.98
Al II	$3s5f\ ^3F$	14 ± 2^d	13.42			12.8
Al II	$3p3d\ ^3F$	3.5 ± 0.3^d	3.96			3.79
Si III	$3p^2\ ^1S$	0.58 ± 0.04^e	0.432		0.40	
Si III	$3s3p\ ^1P$	0.40 ± 0.1^f	0.391		0.39	
Si III	$3p^2\ ^1D$	26 ± 3^f 26 ± 1.5^g	35.21		39.5	
Si III	$3s3d\ ^1D$		0.212		0.22	
Si III	$3s4d\ ^1D$	1.90 ± 0.3^f 1.25 ± 0.15^g	1.20			
Si III	$3s4s\ ^3S$	1.06 ± 0.05^f 0.5 ± 0.1^h	0.421	0.413		
Si III	$3s4p\ ^3P$	4.3 ± 0.5^f 3.3 ± 0.3^g	3.32	3.38		
Si III	$3s3d\ ^3D$	0.36 ± 0.04^f	0.344			
P IV	$3s4s\ ^1S$		0.334	0.357		
P IV	$3s3p\ ^1P$	0.22 ± 0.02^i	0.265		0.26	
P IV	$3p^2\ ^1D$	8.2 ± 0.8^i	10.34		11.9	
P IV	$3s3d\ ^1D$		0.119		0.12	
P IV	$3p3d\ ^1F$		0.162		0.16	
P IV	$3s4s\ ^3S$		0.181	0.178		
P IV	$3s4p\ ^3P$	1.1 ± 0.3^i	1.15	1.14		
S V	$3s4s\ ^1S$		0.161	0.166		
S V	$3s3p\ ^1P$	0.19 ± 0.01^j 0.28 ± 0.01^l	0.196		0.20	0.192 ^k
S V	$3p^2\ ^1D$	5.6 ± 0.5^m	5.14		5.91	
S V	$3s3d\ ^1D$	0.098 ± 0.01^l	0.084		0.085	
S V	$3p3d\ ^1F$		0.085		0.087	

^aReference [43].

^bReference [44].

^cReference [45].

^dReference [46].

^eReference [47].

^fReference [48].

^gReference [49].

^hReference [50].

ⁱReference [51].

^jReference [52].

^kReference [39].

^lReference [53].

^mReference [54].

$3snd$ and the doubly excited $3p4p$, $3d^2$, $3p4f$, and $3p5p^1D$ states in spite of the relatively smooth variation in quantum defect for the $3snd^1D$ series shown in Fig. 4. In addition to the nonuniform variation of the lifetimes as a function of increasing effective quantum numbers, our calculation has also shown that the lifetimes for a specific higher excited $3snd^1D$ state do not necessarily decrease monotonically as Z increases along the isoelectronic sequence. As shown in Fig. 9, the trend of gradual decrease in lifetime is always reversed when an additional doubly excited perturber plunges into the series of singly excited $3snd^1D$ series. Detailed examination of the calculated oscillator strengths also reveals that the radiative lifetime seems to be affected more directly by the oscillator strength redistribution among the upper states due to the neighboring perturbers than the presence of additional decay channels.

The quantitative accuracy of the present CI procedure has been demonstrated recently in the transition probabilities and radiative lifetimes calculation for several di-

valent atoms [18,19]. In Table V, our calculated radiative lifetimes for a few selected low-lying states are compared with some of the existing theoretical [35,36,39–42] and experimental [43–54] results. The agreement is very good in general. More comprehensive numerical results for the excitation energies, the dipole oscillator strengths, and the transition probabilities will be presented elsewhere. The presence of nonuniform variations in radiative lifetimes, along a series of singly excited states for a divalent atom as well as its corresponding isoelectronic sequence, suggests that a detailed and reliable theoretical study should be carried out before a smoothing procedure can be applied based on the limited experimental measurements.

ACKNOWLEDGMENT

This work is supported by the NSF under Grant No. PHY89-03384.

-
- [1] B. Edlén, in *Handbuch der Physik*, edited by S. Flügge (Springer, Berlin, 1964), Vol. 27, p. 80.
- [2] N. Reistad and I. Martinson, *Phys. Rev. A* **34**, 2632 (1986).
- [3] A. Hibbert, *Rep. Prog. Phys.* **38**, 1217 (1975).
- [4] A. Dalgarno, *Nucl. Instrum. Methods* **110**, 183 (1973).
- [5] W. L. Wiese and A. Weiss, *Phys. Rev.* **175**, 50 (1968); M. W. Smith and W. L. Wiese, *Astrophys. J. Suppl. Ser.* **23**, 103 (1971).
- [6] C. Froese Fischer, *Phys. Scr.* **14**, 269 (1976); E. Biémont and M. Godefroid, *ibid.* **18**, 323 (1978).
- [7] T. N. Chang and R. Q. Wang, *Phys. Rev. A* **36**, 3535 (1987).
- [8] C. Froese Fischer and M. Godefroid, *Phys. Scr.* **25**, 394 (1982).
- [9] T. N. Chang and E. T. Bryan, *Phys. Rev. A* **38**, 645 (1988); C. Froese Fischer, *Phys. Scr.* **21**, 466 (1980).
- [10] T. Brage and A. Hibbert, *J. Phys. B* **22**, 713 (1989).
- [11] M. Godefroid and C. Froese Fischer, *Phys. Scr.* **31**, 237 (1985).
- [12] N. Reistad, T. Brage, J. O. Ekberg, and L. Engström, *Phys. Scr.* **30**, 249 (1984).
- [13] J. P. Briand, P. Charles, J. Arianer, H. Laurent, C. Goldstein, J. Dubau, M. Loulergue, and F. Bely-Dubau, *Phys. Rev. Lett.* **52**, 617 (1984).
- [14] R. E. Marrs, M. A. Levine, D. A. Knapp, and J. R. Henderson, *Phys. Rev. Lett.* **60**, 1715 (1988).
- [15] D. J. Wineland and W. M. Itano, *Phys. Today* **40**, (6), 34 (1987).
- [16] S. Chu, J. E. Bjorkholm, A. Ashkin, and A. Cable, *Phys. Rev. Lett.* **57**, 314 (1986).
- [17] M. F. Politis, H. Jouin, M. Bonnefoy, J. J. Bonnet, M. Chassevent, A. Fleury, S. Bliman, and C. Harel, *J. Phys. B* **20**, 2267 (1987); R. Bruch, S. Datz, P. D. Miller, P. L. Pepmiller, H. K. Krause, J. K. Swenson, and N. Stoterfoht, *Phys. Rev. A* **36**, 394 (1987).
- [18] T. N. Chang, *Phys. Rev. A* **41**, 4922 (1990).
- [19] T. N. Chang and X. Tang, *J. Quant. Spectrosc. Radiat. Transfer* **43**, 207 (1990); T. N. Chang and Yi Mu, *ibid.* **44**, 413 (1990).
- [20] T. N. Chang, *Phys. Rev. A* **39**, 4946 (1989); in *Relativistic, Quantum Electrodynamics, and Weak Interaction Effects in Atoms*, edited by W. Johnson, P. Mohr, and J. Sucher, AIP Conf. Proc. No. 189 (AIP, New York, 1989), p. 217.
- [21] T. N. Chang and Y. S. Kim, *Phys. Rev. A* **34**, 2609 (1986).
- [22] C. deBoor, *A Practical Guide to Splines* (Springer, New York, 1978).
- [23] W. R. Johnson, S. A. Blundell, and J. Sapirstein, *Phys. Rev. A* **37**, 307 (1988).
- [24] H. A. Bethe and E. E. Salpeter, *Quantum Mechanics of One- and Two-Electron Atoms* (Plenum, New York, 1977), p. 250.
- [25] T. N. Chang, *Phys. Rev. A* **36**, 447 (1987).
- [26] R. N. Zare, *J. Chem. Phys.* **45**, 1966 (1966); C. Laughlin and G. A. Victor, in *Atomic Physics*, edited by S. J. Smith and G. K. Walters (Plenum, New York, 1973), Vol. 3, p. 247; L. Lipsky and A. Russek, *Phys. Rev.* **142**, 59 (1966); L. Lipsky and M. J. Conneely, *Phys. Rev. A* **14**, 2193 (1976).
- [27] T. N. Chang and R. Q. Wang, *Phys. Rev. A* **43**, 1218 (1991).
- [28] W. C. Martin and R. Zalubas, *J. Phys. Chem. Ref. Data* **8**, 826 (1979).
- [29] W. C. Martin and R. Zalubas, *J. Phys. Chem. Ref. Data* **12**, 347 (1983).
- [30] W. C. Martin and R. Zalubas, *J. Phys. Chem. Ref. Data* **14**, 772 (1985).
- [31] I. Joelsson, P. O. Zetterberg, and C. E. Magnusson, *Phys. Scr.* **23**, 1087 (1981).
- [32] K. Aashamar, T. M. Luke, and J. D. Talman, *Phys. Scr.* **34**, 386 (1986).
- [33] S. S. Tayal and A. Hibbert, *J. Phys. B* **17**, 3835 (1984).
- [34] C. Froese Fischer, *J. Opt. Soc. Am.* **69**, 118 (1979).
- [35] C. Froese Fischer and M. Godefroid, *Nucl. Instrum. Methods* **202**, 307 (1982).
- [36] A. W. Weiss, *J. Chem. Phys.* **47**, 3573 (1967).
- [37] K. L. Baluja and A. Hibbert, *J. Phys. B* **13**, L327 (1980).
- [38] S. S. Tayal, *Phys. Scr.* **32**, 523 (1985).

- [39] K. L. Baluja and A. Hibbert, *Nucl. Instrum. Methods Phys. Res. B* **9**, 477 (1985).
- [40] G. A. Victor, R. F. Stewart, and C. Laughlin, *Astrophys. J. Suppl. Ser.* **31**, 237 (1976).
- [41] K. Aashamar, T. M. Luke, and J. D. Talman, *Phys. Scr.* **37**, 13 (1988).
- [42] A. W. Weiss, *Phys. Rev. A* **9**, 1524 (1974).
- [43] M. E. M. Head, C. E. Head, and J. N. Lawrence, in *Beam-Foil Spectroscopy, Vol. I, Atomic Structure and Lifetimes*, edited by I. A. Sellin and D. J. Pegg (Plenum, New York, 1976), p. 147.
- [44] J. A. Kernahan, E. H. Pinnington, J. A. O'Neill, R. L. Brooks, and K. E. Donnelly, *Phys. Scr.* **21**, 267 (1979).
- [45] H. G. Berry, J. Bromander, and R. Buchta, *Phys. Scr.* **1**, 181 (1970).
- [46] T. Andersen, J. R. Roberts, and G. Sorensen, *Phys. Scr.* **4**, 52 (1971).
- [47] A. E. Livingston, J. A. Kernahan, D. J. G. Irwin, and E. H. Pinnington, *J. Phys. B* **9**, 389 (1976).
- [48] H. G. Berry, J. Bromander, L. J. Curtis, and R. Buchta, *Phys. Scr.* **3**, 125 (1971).
- [49] S. Bashkin, G. Astner, S. Mannervik, P. S. Ramanujam, M. Scofield, S. Huldt, and I. Martinson, *Phys. Scr.* **21**, 820 (1980).
- [50] A. E. Livingston, Y. Baudinet-Robinet, H. P. Garnir, and P. D. Dumont, *J. Opt. Soc. Am.* **66**, 1393 (1976).
- [51] L. J. Curtis, I. Martinson, and R. Buchta, *Phys. Scr.* **3**, 197 (1971).
- [52] N. Reistad, C. Jupén, S. Huldt, L. Engström, and I. Martinson, *Phys. Scr.* **32**, 164 (1985).
- [53] P. D. Dumont, H. P. Garnir, and Y. Baudinet-Robinet, *J. Opt. Soc. Am.* **68**, 825 (1978).
- [54] B. I. Dynefors and I. Martinson, *Phys. Scr.* **17**, 123 (1978).